Girumugisha, G. and Ovalle, C. (2025) ***Géotechnique Letters*** **00**, 000–000, https://doi.org/10.1680/jgele.25.00009

End restraint effects in triaxial tests on H:D = 2:1 specimens of rockfill material

G. GIRUMUGISHA* and C. OVALLE†

Several authors have shown that end restraint effects in triaxial tests are negligible in specimens with a height-to-diameter ratio of H:D≥2. However, these works are mainly based on fine soils and sands, and few studies have focused on coarse angular soils, which typically mobilise high frictional stresses that could boost boundary effects. The aim of this study is to assess end restraint effects in triaxial tests on H:D = 2:1 specimens of rockfill material, through a comprehensive set of drained tests on loose dry samples of 150 mm in diameter. The results show that end restraint effects in coarse angular soil are not overcome in specimens having H:D = 2:1. Standard rough end platens induce higher and more scattered secant strain modulus, dilatancy and shear strength. Thus, lubrication should be systematically used in these materials.

KEYWORDS: end restraint; grading; gravels; rockfill; shear strength; triaxial test

INTRODUCTION

The mechanical characterisation of coarse soils is usually carried out based on tests in small-scaled samples, which may be affected by size effects (Marachi *et al*., 1972; Al-Hussaini, 1983; Hu *et al*., 2011; Girumugisha *et al*., 2026). Recent research has shown that the sources of size effects are mainly related to differences in grading (Muir Wood & Maeda, 2008; Girumugisha *et al*., 2024), particle shape (Linero *et al*., 2017; Ovalle & Dano, 2020; Carrasco *et al*., 2025), particle crushing (Frossard *et al*., 2012; Ovalle *et al*., 2014) and specimen size (Quiroz-Rojo *et al*., 2024; Cantor & Ovalle, 2025). However, test conditions can differ greatly between experimental setups, particularly end restraint effects in triaxial specimens. This topic was early reported in the literature for fine soils and sands (Taylor, 1941; Rowe & Barden, 1964; Bishop & Green, 1965; Duncan & Dunlop, 1968), but has rarely been studied for coarse soils.

In standard triaxial devices, the interface between the soil and the end platens is a rough porous stone, restricting free dilation. Such inherent kinematic constraints induce heterogeneous strain fields (Raju *et al*., 1972; Sheng *et al*., 1997; Frost & Yang, 2003; Liu *et al*., 2013; Peri *et al*., 2019), poor testing repeatability (Colliat-Dangus *et al*., 1988; Mozaffari *et al*., 2022) and uncertainty in critical state (CS) parameters (Lee & Vernese, 1978; Reid *et al*., 2021; Wightman *et al*., 2024).

Taylor (1941) suggested a minimum specimen slenderness to avoid end friction effects, defined as a height-to-diameter ratio H:D ≥ 2. While systematic studies performed in fine soils (Shockley & Ahlvin, 1960; Olson *et al*., 1964; Duncan & Dunlop, 1968; Asaoka *et al*., 1994; Kodaka *et al*., 2007; Muraro & Jommi, 2019) and sands (Olson *et al*., 1964; Rowe & Barden, 1964; Bishop & Green, 1965; Roy & Lo, 1971; Raju *et al*., 1972; Colliat-Dangus *et al*., 1988) have shown consistent shear strength, nonhomogeneous strain fields are not fully overcome with H:D ≥ 2 (Muraro & Jommi, 2019; Mozaffari *et al*., 2022; Yeh *et al*., 2024). Rowe & Barden (1964) proposed enlarged end platens covered with a greased latex rubber sheet. However, slender lubricated specimens often slide sideways and buckle at large strains (Olson *et al*., 1964; Rowe & Barden, 1964; Duncan & Dunlop, 1968), which can be avoided using H:D ≈ 1 (Hettler & Vardoulakis, 1984; Goto & Tatsuoka, 1988; Feda *et al*., 1993). The only study on the effects of triaxial end restraint in rockfill was reported by Al-Hussaini (1970). His results indicated that rough end platens significantly enhance the stiffness and dilatancy, while having a minor effect on shear strength. Although most testing standards have been drawn based on test results in fine soils and sands with CS friction angle lower than $\varphi' \sim 35°$, data in coarse soils are scarce. Provided that coarse angular soils typically exhibit high values of $\varphi' \sim 40^{\circ}$ or more (Leps, 1970; Ovalle *et al*., 2020), it can be expected that frictional components at the specimen boundaries might have a great impact on the material response.

The main objective of this letter is to assess end restraint effects in triaxial tests on H:D = 2:1 specimens of coarse angular soil. Monotonic triaxial tests were performed on dry samples of D = 150 mm, under consolidated drained conditions at confining stresses of $\sigma_3 = 100$ and 400 kPa. The results with rough and enlarged lubricated platens are compared. In addition, the effects of grading were studied on scaled samples prepared by scalping and parallel grading techniques.

METHODOLOGY

Materials tested

Well-graded rockfill material was sampled from a quarry in St-Eustache, Canada. The material consists of blasted and crushed dolomite rock, with specific gravity $G_s = 2.75$ and subangular grain shapes. Field particle size distribution (PSD) shown in Fig. 1 indicates well-graded gravel without fines (GW) according to ASTM (2017). Maximum particle size is $d_{max} = 90$ mm, $d_{50} = 13{\cdot}9$ mm and uniformity and curvature coefficients are given by $C_u = d_{60}/d_{10} = 9$ and $C_c = (d_{30})^2/(d_{10}d_{60}) = 1{\cdot}6$, respectively.

Manuscript received 28 January 2025; accepted 16 February 2026.

*Department of Civil, Geological and Mining Engineering, Polytechnique Montreal, Quebec, Canada.
†Research Institute on Mines and Environment (RIME) UQAT-Polytechnique, Quebec, Canada (corresponding author: carlos.ovalle@polymtl.ca).

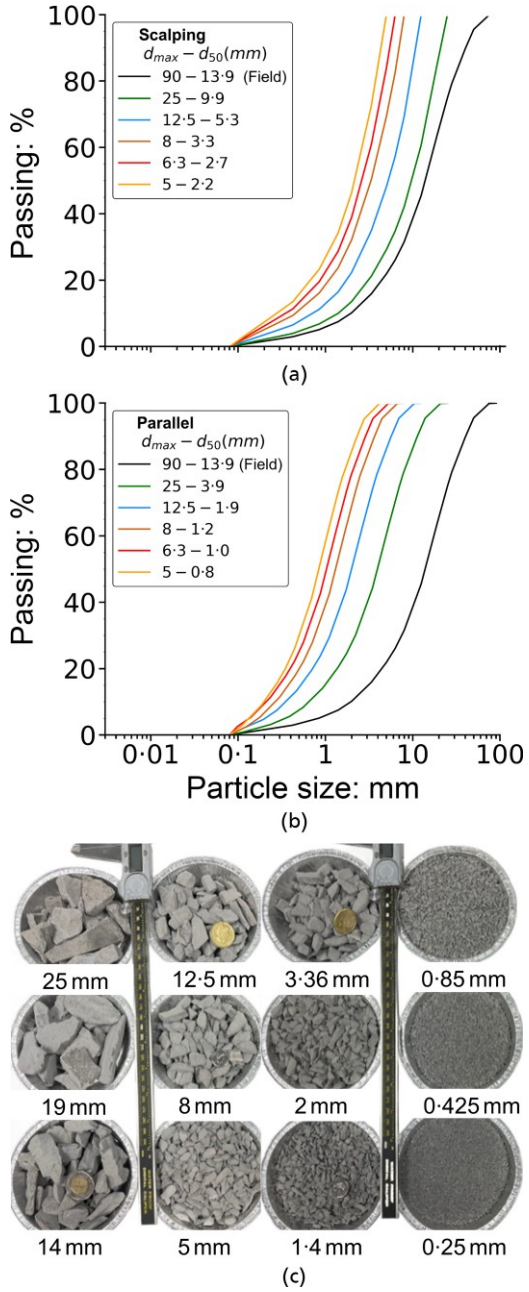

Fig. 1. Field and scaled samples of quarried rockfill, scaling with d_{max} between 5 and 25 mm using (a) scalping grading and (b) parallel grading techniques; (c) characteristic photos of the subangular particles

Several samples were prepared using scalping (S) (Fig. 1(a)) and parallel grading (P) (Fig. 1(b)) techniques; d_{max} of different scaled materials was set to 5, 6, 8, 12 and 25 mm. For S samples, particles coarser than a chosen d_{max} were simply removed and a new PSD was generated. P samples were prepared by creating a parallel PSD curve between percents passing of 100% to 10%; for size fractions finer than d_{10}, the PSD curves were simply extended until the finest particle in the field material ($d_{min} = 0.08$ mm). The detailed information of all the materials is given in Table S1, included as supplementary information.

Specimens preparation

Specimens were prepared in a mould of H:D = 300/150 mm, covered by a 2-mm-thick latex membrane. D is in accordance with ASTM (2020) which stipulates a maximum ratio D/d_{max} of 6. To minimise strain localisation promoted in dense soils, all the specimens were prepared in the loosest possible configuration, by pouring the material in layers without any compaction. Ten distinct layers of homogeneous dry material (≈950 g each) were gently placed in the mould. Due to different grading between samples, the attained dry densities varied slightly from $\gamma_d = 16.14 - 17.64\,kN/m^3$ in S and $\gamma_d = 16.40 - 18.12\,kN/m^3$ in P samples (see Table S1).

Two lubricated end configurations were evaluated, both with enlarged caps of 170 mm in diameter and made of 3-cm-thick lucite material (see Fig. 2). The aim was to evaluate the best approach that avoids buckling (Raju *et al.*, 1972; Sheng *et al.*, 1997). The first configuration consists of a thin film of silicone grease applied to the entire section of the enlarged caps, covered by a continuous sheet of latex membrane (1 mm thick). For the second lubricated configuration, a cross-shaped cut was introduced in the centre of the latex sheet, as proposed by Feda *et al.* (1993), to prevent the membrane from restricting radial expansion (see Fig. 2(b)).

Triaxial testing

Specimens were isotropically consolidated until volume stabilisation (≈45 min). Two effective confining pressures of $\sigma'_3 = 100$ and 400 kPa were used. Since the specimens were dry, their volumetric strains (ε_v) were estimated through the volume changes of the confinement cell. Shearing was carried out at constant axial strain rate of 0·3%/min (ASTM, 2020). The deviatoric stress $q = \sigma'_1 - \sigma'_3$ and the mean effective stress $p' = (\sigma'_1 + 2\sigma'_3)/3$ were monitored until reaching an axial strain of $\varepsilon_a = 15\%$.

The following tests were carried out: (i) 30 tests on specimens with standard rough ends and (ii) 49 tests with enlarged platens and lubricated sheets (Fig. 2).

EXPERIMENTAL RESULTS

Figure 3 displays photos of the specimens after testing. Regarding specimens with rough ends (Fig. 3(a)), localised failure and specimen bulging are systematically observed. This is an unexpected result in such loose materials, and suggests that end restraint effects might be amplified in highly frictional soils, such as coarse crushed rock. Most of the cases with a continuous lubricated sheet exhibited buckling and sideways sliding, as qualitatively shown in Fig. 3(b). On the other hand, cross cutting the sheets helps to maintain the verticality of the specimens (see Fig. 3(c)), certainly because this setup facilitates radial movement of

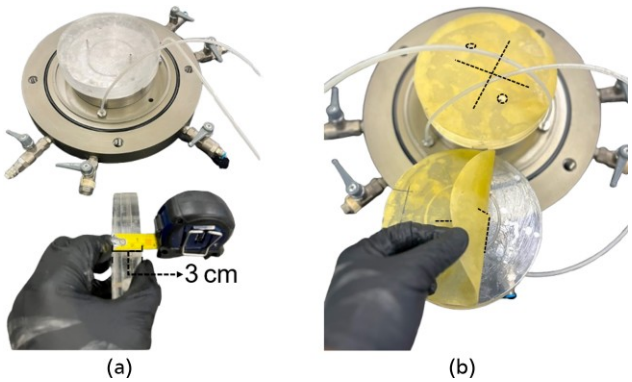

Fig. 2. Enlarged cap setup (D = 170 mm): (a) lubricated cap; (b) positioning cross-cut greased rubber sheets

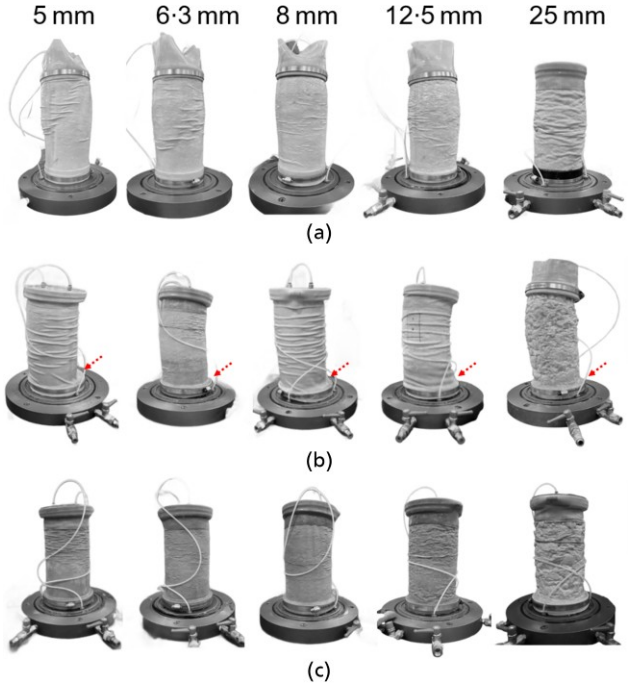

Fig. 3. Pictures qualitatively illustrating specimen deformation after testing for each tested d_{max}. (a) Standard rough ends. (b) Lubricated with continuous greased latex rubber sheets; red arrows designate sliding movement. (c) Lubricated with cross-cut greased latex rubber sheets

the particles in contact with the caps. Given these results, all tests with continuous sheets were repeated using cross-cut sheets, and the following analyses consider only the latter configuration.

Figure 4 presents typical stress–strain responses for selected S and P materials (d_{max} = 12·5 mm), tested with rough (R) and lubricated platens (L), where the stress ratio q/p' and ε_v are plotted against ε_a.

Following the same trend of the specimens with d_{max} =12·5 mm shown in Fig. 4, all the tests exhibit stress hardening towards maximum q/p' reached around ε_a = 15%. The stress–strain plots of the 79 tests are included as supplementary information: Figs. S1 and S2 for S and P samples, respectively. Tests with standard rough ends overestimate $(q/p')_{max}$ values and dilation in both sets of materials (S and P) and confining stresses. However, these differences are greatly reduced at higher σ'_3. To highlight these observations, Fig. 5 presents the variation of ϕ' in all the tests, with $sin\phi' = 3(q/p')_{max}/(6 + (q/p')_{max})$; the results are plotted against d_{50}, displaying all the tests carried out on every PSD shown in Fig. 1 (detailed data in Table S1). Note that datapoints sharing the same marker for a given d_{50} correspond to test repetitions. Since the normalised critical strength does not depend on PSD (Muir Wood & Maeda, 2008; Li *et al.*, 2013; Yang & Luo, 2018; Cantor & Ovalle, 2025), ϕ' should be a stable value among all the samples tested, provided that boundary effects are negligible. For all tests with rough ends, ϕ' is scattered between 39·6° and 46·4° at σ'_3 = 100 kPa, and 38·8°–41·7° at 400 kPa, without a clear distinction between the SR and PR tests. On the other hand, lubricated tests exhibited slightly lower strength between ϕ' =39·2°–43·5° at σ'_3 = 100 kPa and 37·3°–40·7° at 400 kPa, with less scattering compared to the cases with rough ends. These relatively high values of φ′ – compared with sands and fine soils – are consistent with enhanced end restraint effects, as hypothesised in the first section of this letter.

Figure 6 displays the maximum dilatancy rates ($(d\varepsilon_v/d\varepsilon_a)_{max}$; negative values designate dilation) for all tests. As expected, the results reflect that rough boundaries promote dilatancy and increase dispersion of the data. The

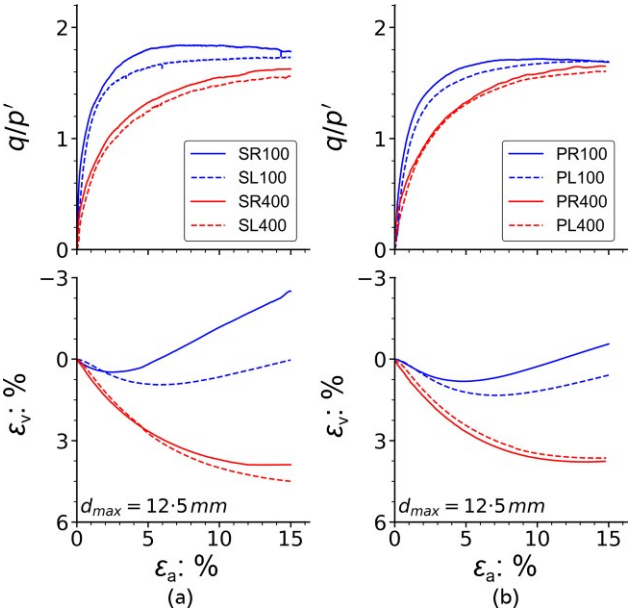

Fig. 4. Stress–strain behaviour of specimens of d_{max} = 12·5 mm, with standard rough (continuous lines) and lubricated ends (dashed lines) at 100 (blue) and 400 kPa (red), respectively: (a) S and (b) P materials; the first letter in the legend indicates the PSD scaling method (S or P), while the second one designates the platen configuration (R or L); the number that follows is σ'_3 in kPa

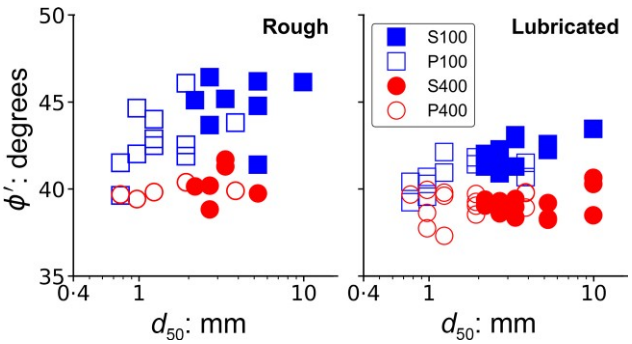

Fig. 5. The variation of the mobilised ϕ' with d_{50}: blue square and *red* circle filled and empty markers for S and P samples, respectively

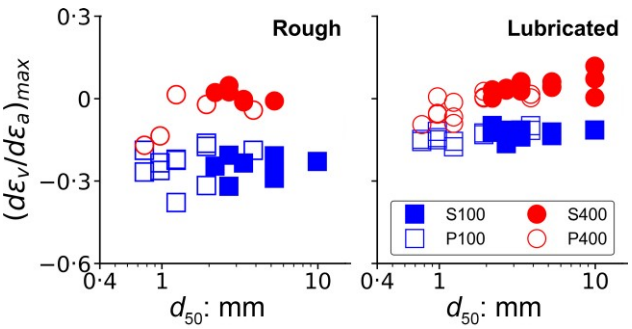

Fig. 6. The variation of $(d\varepsilon_v/d\varepsilon_a)_{max}$ with d_{50}: *blue* square and *red* circle filled and empty markers for S and P samples, respectively

main source of scattering in R cases is probably related to strain localisation, as qualitatively shown in Fig. 3(a). In such heterogeneous strain fields, ε_v does not necessarily represent the specimen strain, but a mean value between volume change during shear sliding within the localised shear band, and a relatively constant volume in the rest of the specimen.

Figure 7 presents the characteristic secant strain modulus (E_{50}) variation across d_{50} for all tests; E_{50} is defined as the ratio of the 50% of the maximum deviatoric stress and the corresponding ε_a. In SR and PR cases, E_{50} exhibits great scattering without a noticeable trend. Moreover, the values appear to increase with the particle size in tests at $\sigma'_3 = 100$ kPa (from ≈8 to 19 MPa), while the inverse trend is observed at 400 kPa (from ≈23 to 17 MPa). Comparatively, E_{50} of specimens with lubricated platens exhibit more stable results in all materials S and P.

Due to the classical strain limitations of the triaxial test setup, the specimens did not fully reach CS. Nevertheless, Fig. 8 shows that the tendency displayed on Fig. 6 persists at the end of each test ($\varepsilon_a = 15\%$): the R configuration exhibits enhanced dilatancy rate and greater variability compared to L. While this study does not permit definitive conclusions regarding the influence of end restraint on CS, the results clearly indicate that boundary effects persist at large strains.

In order to assess the representativeness and test repeatability of small scaling methods, Fig. 9 summarises the results by displaying the mean values and their standard deviation for each testing condition (R and L) and scaling technique (S and P). In terms of shear strength (Fig. 9(a)), rough ends clearly give higher mean φ′, particularly at $\sigma'_3 = 100$ kPa. The difference in ϕ' between 100 and 400 kPa is remarkably reduced in PL tests, indicating

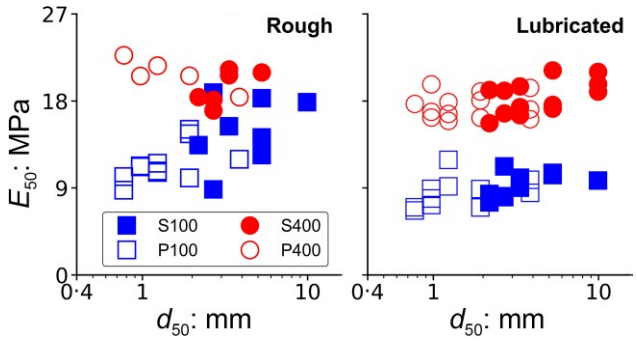

Fig. 7. The variation of E_{50} with d_{50}: *blue* square and *red* circle filled and empty markers for S and P samples, respectively

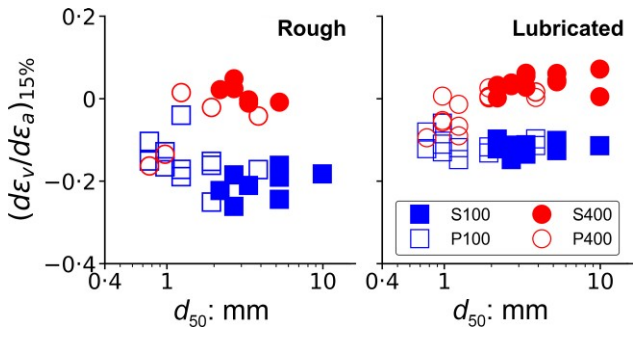

Fig. 8. The variation of $(d\varepsilon_v/d\varepsilon_a)$ at $\varepsilon_a = 15\%$ with d_{50}: *blue* square and *red* circle filled and empty markers for S and P samples, respectively

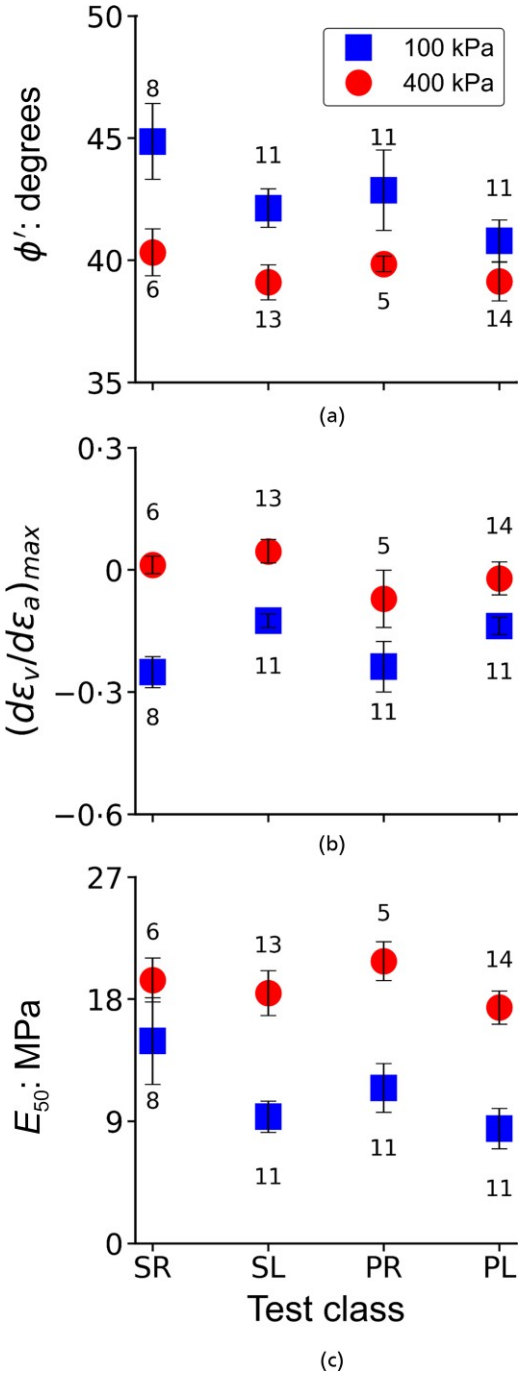

Fig. 9. Summary of mean values and standard deviations of (a) ϕ', (b) $(d\varepsilon_v/d\varepsilon_a)_{max}$ and (c) E_{50}, for all tests; marks represent mean values, bars are the standard deviations and numbers next to each mark indicate the number of tests carried out

that lubrication and better graded materials give more stable results. The average ϕ' and its standard deviation for SR and PL at $\sigma'_3 = 100$ kPa are $\phi' = 44.9 \pm 1.5^\circ$ and $40.8 \pm 0.9^\circ$, respectively. At $\sigma'_3 = 400$ kPa, these differences are reduced to $\phi' = 40.3 \pm 0.3^\circ$ and $39.1 \pm 0.8^\circ$ for SR and PL, respectively. Regarding dilatancy (Fig. 9(b)), the differences due to end friction effects are noticeable only at $\sigma'_3 = 100$ kPa, with enhanced $|(d\varepsilon_v/d\varepsilon_a)_{max}|$ in R specimens. On the other hand, mean E_{50} values increase with rough ends, particularly in S samples (Fig. 9(c)). On average, $E_{50} = 14.9 \pm 3.2$ and 8.5 ± 1.5 MPa for SR and PL at $\sigma'_3 = 100$ kPa, respectively, and $E_{50} = 19.4 \pm 1.6$ and 17.4 ± 1.2 MPa at 400 kPa.

DISCUSSION

Since this study did not include local strain measurements during shearing, the results are treated as a boundary-value problem, and only macro-mechanical values were quantified (i.e. at the specimen scale). Nevertheless, qualitative observations of strain heterogeneity at the end of the tests are consistent with the trends observed in data scatter and test repeatability. Future research should include meso- and micro-scale strain evaluations using image analysis techniques (Alshibli *et al.*, 2003; Sachan & Penumadu, 2007). This would enable assessing the contribution of coarse angular particles to end restraint effects.

The relatively high shear strength of rockfill materials is largely attributed to the interlocking mechanism of angular grains (Charles & Watts, 1980; Barton & Kjærnsli, 1981). This phenomenon is fundamentally a kinematic constraint on grain rotation that arises from particle angularity, as demonstrated experimentally (Fonseca *et al.*, 2013) and supported by numerical studies (Azéma & Radjaï, 2010). These constraints develop column-like force chains upon strain hardening (Kuhn & Bagi, 2004), which may buckle and lead to enhanced dilatancy (Iwashita & Oda, 1998). While such load-bearing structures are inherent to the mechanical behaviour of angular rockfill, the additional kinematic constraints imposed by end restraint may artificially promote their development, potentially resulting in an overestimation of their contribution to dilatancy. A perspective of this study could be to track and identify particle-scale mechanisms near the specimen ends using micro-CT scanning. These direct observations may shed light on the origin of the pronounced end restraint effects observed in highly angular materials.

CONCLUSIONS

The following conclusions are drawn:

- Unlike fine-grained soils and sands, end restraint effects in triaxial specimens of scaled rockfill materials are not fully overcome with slenderness H:D = 2:1.
- End restraint effects appear as higher and scattered shear strength, dilatancy and secant stiffness.
- Samples prepared by scalping and tested with standard rough platens revealed the strongest end friction effects, with higher values of ϕ' and E_{50} compared with parallel graded materials under the same testing conditions.
- In general, parallel graded samples with lubricated caps displayed relatively consistent strain–strain curves in the whole set of tests, particularly at high confining pressure.

The results indicate that end lubrication and shredded sheets on lubricated caps should be systematically used in triaxial tests on H:D = 2:1 specimens of coarse rockfill materials. While these recommendations provide valuable guidance for practitioners, the findings of the study opens perspectives to wider research. Specifically, end restraint effects on nonuniform deformation of rockfill triaxial specimens should be quantified through advanced experimental methods. This might allow for evaluating how particle shape and size influence the material response in relation to boundary conditions.

ACKNOWLEDGEMENTS

This study was funded by the Natural Sciences and Engineering Research Council of Canada (NSERC) [reference RGPIN-2019-06118] and the industrial partners of the Research Institute on Mines and the Environment (RIME) (http://www.irme.ca/en). The authors also thank Lafarge Canada for providing rockfill material and Patrick Bernèche for his support in the extensive experimental work.

REFERENCES

Al-Hussaini, M. M. (1970). The influence of end restraint and method of consolidation on the drained triaxial compressive strength of crushed Napa basalt. In *Miscellaneous Paper S-70-18, U.S. Army Engineer Waterways Experiment Station* Vicksburg, Mississippi, USA.

Al-Hussaini, M. M. (1983). Effect of particle size and strain conditions on the strength of crushed basalt. *Can Geotech J* **20**, No. 4, 706–717, 10.1139/t83-077.

Alshibli, K. A., Batiste, S. N. & Sture, S. (2003). Strain localization in sand: Plane strain versus triaxial compression. *J Geotech Geoenviron Eng* **129**, No. 6, 483–494, 10.1061/(ASCE)1090-0241(2003)129:6(483).

Asaoka, A., Nakano, M. & Noda, T. (1994). Soil-water coupled behaviour of saturated clay near/at critical state. *Soils and foundations* **34**, No. 1, 91–105, 10.3208/sandf1972.34.91.

ASTM. (2017). ASTM D2487 Standard practice for classification of soils for engineering purposes (Unified Soil Classification System). ASTM International, West Conshohocken.

ASTM. (2020). ASTM D7181 Standard test method for consolidated drained triaxial compression test for soils. ASTM International, West Conshohocken.

Azéma, E. & Radjaï, F. (2010). Stress-strain behavior and geometrical properties of packings of elongated particles. *Phys Rev E Stat Nonlin Soft Matter Phys* **81**, No. 5, 051304, 10.1103/PhysRevE.81.051304.

Barton, N. & Kjærnsli, B. (1981). Shear strength of rockfill. *J Geotech Engrg Div* **107**, No. 7, 873–891, 10.1061/AJGEB6.0001167.

Bishop, A. W. & Green, G. E. (1965). The influence of end restraint on the compression strength of a cohesionless soil. *Géotechnique* **15**, No. 3, 243–266, 10.1680/geot.1965.15.3.243.

Cantor, D. & Ovalle, C. (2025). Sample size effects on the critical state shear strength of granular materials with varied gradation and the role of column-like local structures. *Géotechnique* **75**, No. 1, 29–40, 10.1680/jgeot.23.00032.

Carrasco, S., Cantor, D., Ovalle, C. & Dubois, F. (2025). Particle shape distribution effects on the critical strength of granular materials. *Comput Geotech* **177**, 106896, 10.1016/j.compgeo.2024.106896.

Charles, J. A. & Watts, K. S. (1980). The influence of confining pressure on the shear strength of compacted rockfill. *Géotechnique* **30**, No. 4, 353–367, 10.1680/geot.1980.30.4.353.

Colliat-Dangus, J., Desrues, J. & Foray, P. (1988). Triaxial testing of granular soil under elevated cell pressure. In *Advanced Triaxial Testing of Soil and Rock*, p. 21: ASTM International, 10.1520/STP29082S.

Duncan, J. M. & Dunlop, P. (1968). The significance of cap and base restraint. *J Soil Mech and Found Div* **94**, No. 1, 271–290, 10.1061/JSFEAQ.0001087.

Feda, J., Bohac, J. & Herle, I. (1993). End restraint in triaxial testing of soils. *Acta Technica CSAV* **38**, 197.

Fonseca, J., O'sullivan, C., Coop, M. R. & Lee, P. D. (2013). Quantifying the evolution of soil fabric during shearing using scalar parameters. *Géotechnique* **63**, No. 10, 818–829, 10.1680/geot.11.P.150.

Frossard, E., Hu, W., Dano, C. & Hicher, P.-Y. (2012). Rockfill shear strength evaluation: a rational method based on size effects. *Géotechnique* **62**, No. 5, 415–427, 10.1680/geot.10.P.079.

Frost, J. D. & Yang, C.-T. (2003). Effect of end platens on microstructure evolution in dilatant specimens. *Soils Found.* **43**, No. 4, 1–11, 10.3208/sandf.43.4_1.

Girumugisha, G., Ovalle, C. & Ouellet, S. (2024). Grading scalping and sample size effects on critical shear strength of mine waste rock through laboratory and in-situ testing. *Int. J. Rock Mech. Min. Sci.* **183**, 105915, 10.1016/j.ijrmms.2024.105915.

Girumugisha, G., Ovalle, C., Reith, H. & Stutz, H. H. (2026). Effects of triaxial sample scaling on the mechanical behavior

of alluvial gravels. *J Geotech Geoenviron Eng* **152**, No. 1, 10.1061/JGGEFK.GTENG-13923.

Goto, S. & Tatsuoka, F. (1988). Effects of end conditions on triaxial compressive strength for cohesionless soil. In *Advanced Triaxial Testing of Soil and Rock*, pp. 14: ASTM International, 10.1520/STP29108S.

Hettler, A. & Vardoulakis, I. (1984). Behaviour of dry sand tested in a large triaxial apparatus. *Géotechnique* **34**, No. 2, 183–197, 10.1680/geot.1984.34.2.183.

Hu, W., Dano, C., Hicher, P.-Y., Le Touzo, J.-Y., Derkx, F. & Merliot, E. (2011). Effect of sample size on the behavior of granular materials. *Geotechnical Testing Journal* **34**, No. 3, 186–197, 10.1520/gtj103095.

Iwashita, K. & Oda, M. (1998). Rolling resistance at contacts in simulation of shear band development by DEM. *J Eng Mech* **124**, No. 3, 285–292, 10.1061/(ASCE)0733-9399(1998)124:3(285).

Kodaka, T., Higo, Y., Kimoto, S. & Oka, F. (2007). Effects of sample shape on the strain localization of water-saturated clay. *Num Anal Meth Geomechanics* **31**, No. 3, 483–521, 10.1002/nag.585.

Kuhn, M. R. & Bagi, K. (2004). Contact rolling and deformation in granular media. *Int J Solids Struct* **41**, No. 21, 5793–5820, 10.1016/j.ijsolstr.2004.05.066.

Lee, K. L. & Vernese, F. J. (1978). End restraint effects on cyclic triaxial strength of sand. *J Geotech Engrg Div* **104**, No. 6, 705–719, 10.1061/AJGEB6.0000644.

Leps, T. M. (1970). Review of shearing strength of rockfill. *J Soil Mech and Found Div* **96**, No. 4, 1159–1170, 10.1061/JSFEAQ.0001433.

Li, G., Ovalle, C., Dano, C. & Hicher, P.-Y. (2013). Influence of grain size distribution on critical state of granular materials. In *Constitutive Modeling of Geomaterials*, pp. 207–210. Berlin, Heidelberg: Springer Berlin Heidelberg.

Linero, S., Fityus, S., Simmons, J., Lizcano, A. & Cassidy, J. (2017). Trends in the evolution of particle morphology with size in colluvial deposits overlying channel iron deposits. *EPJ Web Conf.* **140**, 14005, 10.1051/epjconf/201714014005.

Liu, X., Shao, L. & Guo, X. (2013). Local data analysis for eliminating end restraint of triaxial specimen. *Trans Tianjin Univ* **19**, No. 5, 372–380, 10.1007/s12209-013-2000-1.

Marachi, N. D., Chan, C. K. & Seed, H. B. (1972). Evaluation of properties of rockfill materials. *Journal of the Soil Mechanics and Foundations Division* **98**, No. 1, 95–114, 10.1061/JSFEAQ.0001735.

Mozaffari, M., Liu, W. & Ghafghazi, M. (2022). Influence of specimen nonuniformity and end restraint conditions on drained triaxial compression test results in sand. *Can Geotech J* **59**, No. 8, 1414–1426, 10.1139/cgj-2021-0505.

Muir Wood, D. & Maeda, K. (2008). Changing grading of soil: effect on critical states. *Acta Geotech* **3**, No. 1, 3–14, 10.1007/s11440-007-0041-0.

Muraro, S. & Jommi, C. (2019). Implication of end restraint in triaxial tests on the derivation of stress–dilatancy rule for soils having high compressibility. *Can Geotech J* **56**, No. 6, 840–851, 10.1139/cgj-2018-0343.

Olson, R. E., Campbell, L. M., Lee, K., Seed, H. B., Turnbull, J. M. & Poulos, S. (1964). Discussion of "importance of free ends in triaxial testing". *J Soil Mech and Found Div* **90**, No. 6, 167–179, 10.1061/JSFEAQ.0000670.

Ovalle, C., Frossard, E., Dano, C., Hu, W., Maiolino, S. & Hicher, P.-Y. (2014). The effect of size on the strength of coarse rock aggregates and large rockfill samples through experimental data. *Acta Mech* **225**, No. 8, 2199–2216, 10.1007/s00707-014-1127-z.

Ovalle, C. & Dano, C. (2020). Effects of particle size–strength and size–shape correlations on parallel grading scaling. *Géotechnique Letters* **10**, No. 2, 191–197, 10.1680/jgele.19.00095.

Ovalle, C., Linero, S., Dano, C., Bard, E., Hicher, P.-Y. & Osses, R. (2020). Data compilation from large drained compression triaxial tests on coarse crushable rockfill materials. *J Geotech Geoenviron Eng* **146**, No. 9, 06020013, 10.1061/(ASCE)GT.1943-5606.0002314.

Peri, E., Ibsen, L. B. & Nordahl Nielsen, B. (2019). Influence of sample slenderness and boundary conditions in triaxial test – a review. *E3S Web Conf.* **92**, 02009, 10.1051/e3sconf/20199202009.

Quiroz-Rojo, P., Cantor, D., Renouf, M., Ovalle, C. & Azéma, E. (2024). Rev assessment of granular materials with varied grading based on macro- and micro-mechanical statistical data. *Acta Geotech* **20**, No. 4, 1585–1598, 10.1007/s11440-024-02498-3.

Raju, V., Sadasivan, S. & Venkataraman, M. (1972). Use of lubricated and conventional end platens in triaxial tests on sands. *Soils Found.* **12**, No. 4, 35–43.

Reid, D., Fourie, A., Ayala, J. L., Dickinson, S., Ochoa-Cornejo, F., Fanni, R., Garfias, J., da Fonseca, A. V., Ghafghazi, M., Ovalle, C., Riemer, M., Rismanchian, A., Olivera, R. & Suazo, G. (2021). Results of a critical state line testing round robin programme. *Geotechnique* **71**, No. 7, 616–630, 10.1680/jgeot.19.P.373.

Rowe, P. W. & Barden, L. (1964). Importance of free ends in triaxial testing. *J Soil Mech and Found Div* **90**, No. 1, 1–27, 10.1061/JSFEAQ.0000586.

Roy, M. & Lo, K. (1971). Effect of end restraint on high pressure tests of granular materials. *Can Geotech J* **8**, No. 4, 579–588, 10.1139/t71-059.

Sachan, A. & Penumadu, D. (2007). Strain localization in solid cylindrical clay specimens using digital image analysis (DIA) technique. *Soils Found.* **47**, No. 1, 67–78, 10.3208/sandf.47.67.

Sheng, D., Westerberg, B., Mattsson, H. & Axelsson, K. (1997). Effects of end restraint and strain rate in triaxial tests. *Comput Geotech* **21**, No. 3, 163–182, 10.1016/S0266-352X(97)00021-9.

Shockley, W. G. & Ahlvin, R. G. (1960). Nonuniform conditions in triaxial test specimens. In *Research conference on shear strength of cohesive soils*, ASCE, pp. 341–357.

Taylor, D. (1941). Cylindrical compression research program on stress-deformation and strength characteristics of soils. In *MIT 7th Progress Report to Water Experiments Station*.

Wightman, A., Dickinson, S., Jeong, C.-G., Shanmugarajah, T. & Billings, M. (2024). Importance of sample height–diameter ratio in triaxial testing with free ends for determination of the critical state of sands. *Geotechnical Testing Journal* **48**, No. 2, 147–165, 10.1520/GTJ20240055.

Yang, J. & Luo, X. D. (2018). The critical state friction angle of granular materials: does it depend on grading? *Acta Geotech* **13**, No. 3, 535–547, 10.1007/s11440-017-0581-x.

Yeh, F.-H., Ge, L., Jhuo, Y.-S. & Chen, L.-C. (2024). Re-examining the influence of end restraint on mechanical behaviors of dense quartz sands. *KSCE Journal of Civil Engineering* **28**, No. 6, 2201–2209, 10.1007/s12205-024-1303-1.